

56-33
160520

N 9 3 - 2 7 7 3 2

p-15

A Study of Subterahertz HEMT Monolithic Oscillators *

Youngwoo Kwon and Dimitris Pavlidis
Center for Space Terahertz Technology
Solid State Electronics Laboratory

Department of Electrical Engineering and Computer Science
The University of Michigan, Ann Arbor, MI 48109-2122, USA

Abstract

A detailed study of monolithic InP-based HEMT oscillators for subterahertz operation is presented. InAlAs/InGaAs HEMT's have been optimized for high frequency operation and showed very high maximum oscillation frequencies (f_{max}) of 310 GHz using offset self-aligned Γ -gate technology. Power characteristics of HEMT oscillators are reported. An oscillation power of more than 10 mW was evaluated by large-signal analysis at 320 GHz using HEMT's with $f_{max} = 450$ GHz, $V_{br} = 10$ V and a gate width (W_g) of $8 \times 22.5 \mu m$. Oscillator topology studies showed that complex feedback schemes such as dual and active feedback enhance the negative resistance. Push-push oscillator designs based on harmonic signal generation can finally be used to overcome the frequency barrier imposed by f_{max} .

1 Introduction

InAlAs/InGaAs HEMT's have shown excellent high frequency characteristics and operation capability as discrete devices. A current gain cut-off frequency (f_T) of 305 GHz [1] and a maximum oscillation frequency of 455 GHz have been reported using heterostructures of this type [2]. These very encouraging discrete device results indicate that InP-based HEMT's can be used to realize monolithic circuits with operation frequency well into the millimeter-wave region. A number of such monolithic integrated

*Work supported by NASA under contract NAGW-1334

circuits have recently been demonstrated by the authors. These include monolithic HEMT mixers at 94 GHz showing conversion gain of 1 dB [3] and HEMT doublers at 180 GHz with a conversion loss of 6 dB [4]. Monolithic HEMT oscillators also have been realized by the authors up to W-band showing more than 1 mW power with devices having 36 μm gate periphery [5].

Another possibility opened to HEMT technology is its use for space-based remote sensing and radiometry, where fundamental sources are required to operate above 100 GHz. A first detailed study concerning the power characteristics and the upper frequency limit of InAlAs/InGaAs HEMT's when used as oscillators, has recently been presented by the authors [6]. This paper provides further details on related issues of HEMT use for signal generation. It addresses first the ways of further optimization of InP-based HEMT technology in view of obtaining enhanced f_{max} performance (Section 2). Power and frequency characteristics of monolithic oscillators evaluated with the help of a large-signal analysis are presented in Section 3. Finally, specific designs and topologies of 160 GHz fundamental monolithic HEMT oscillators are discussed in Section 4.

2 Device Optimization for High f_{max}

A very high f_{max} of several hundred gigahertz is necessary to guarantee the device operation as oscillator at millimeter-wave frequencies. Optimization for high f_{max} can be achieved by reducing the parasitic resistances and capacitances of the HEMT. The parasitic source resistance (R_s) consists of two parts : one coming from the contact region (R_c) and the other from the ungated region between the gate and source. In an attempt to minimize the ungated region resistance, a self-aligned gate technology has been applied to InAlAs/InGaAs HEMT's [7]. The ungated region between source and gate has been reduced in this case to less than 0.2 μm and the source access resistance was minimized, resulting in a very high extrinsic f_T of 250 GHz. Although f_{max} is directly proportional to

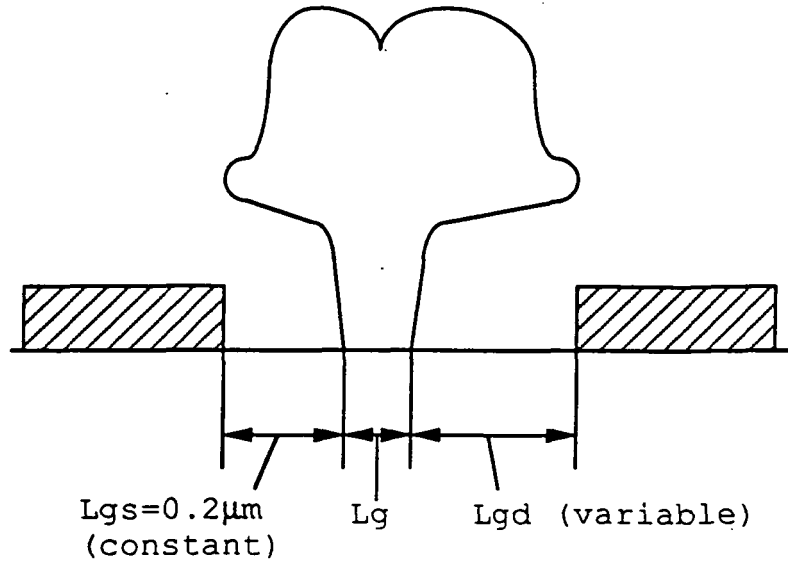


Figure 1: Schematic view of the self-aligned offset Γ gate HEMT

f_T , it was limited in this case due to the high output conductance (G_{ds}) and gate-to-drain capacitance (C_{gd}); this was caused by the proximity of the gate and drain making G_{ds} and C_{gd} higher than in HEMT's fabricated by conventional technology.

A better insight to the problem can be obtained by examining the f_{max} expression which is given by [8]:

$$\frac{f_{max}}{f_T} = \left\{ 4 \frac{G_{ds}}{G_m} \left(G_m R_i + \frac{R_s + R_g}{1/G_m + R_s} \right) + \frac{4}{5} \frac{C_{gd}}{C_{gs}} \left(1 + 2.5 \frac{C_{gd}}{C_{gs}} \right) (1 + G_m R_s)^2 \right\}^{-\frac{1}{2}}$$

It is obvious from Eq. (1) that a high f_{max}/f_T ratio can be achieved by increasing both C_{gs}/C_{gd} and G_m/G_{ds} . These two ratios are related to L_{gd}/L_{gs} , where L_{gs} is the distance between gate and source, and L_{gd} is the distance between gate and drain. L_{gd}/L_{gs} can be increased by offsetting the gate instead of placing it at the center of the source-to-drain region. The novel self-aligned offset Γ -gate developed by the authors [9] and employed in the analysis presented here, allows one to satisfy these requirements. An additional feature of this approach is that L_{gd} and L_{gs} can be controlled much more accurately in this way than in processes where the gate has to be offset aligned between two ohmic contacts. Various L_{gd} values ranging from $0.2 \mu m$ to $0.6 \mu m$ were employed while L_{gs}



Figure 2: SEM photograph of self-aligned offset Γ -gate ($L_{gd} = 0.6 \mu m$)

was fixed at $0.2 \mu m$ as shown in Fig. 1.

The devices were fabricated following the self-aligned process described in [9]. The SEM photograph of the completed gate after the ohmic metal deposition is shown in Fig. 2. The highest f_{max} values were obtained with $L_{gd} = 0.4 \mu m$ and the corresponding microwave results are shown in Fig. 3. f_T is in this case around 150 GHz and f_{max} is greater than 300 GHz. By increasing L_{gd} further, the value of f_{max}/f_T increases due to the higher C_{gs}/C_{gd} and G_m/G_{ds} ratios. However, the magnitude of f_T becomes smaller with L_{gd} due to the increased gate length and source-to-drain spacing. The increase of f_{max}/f_T ratio with L_{gd} is thus compensated by the decrease of f_T and the maximum f_{max} occurs for $L_{gd} = 0.4 \mu m$.

Further f_{max} optimization is expected by reducing the gate length of the devices which had large offsets; due to the increased number of line scans for highly offset gates, the gate length becomes larger than in the case of the symmetric/centered realizations. This

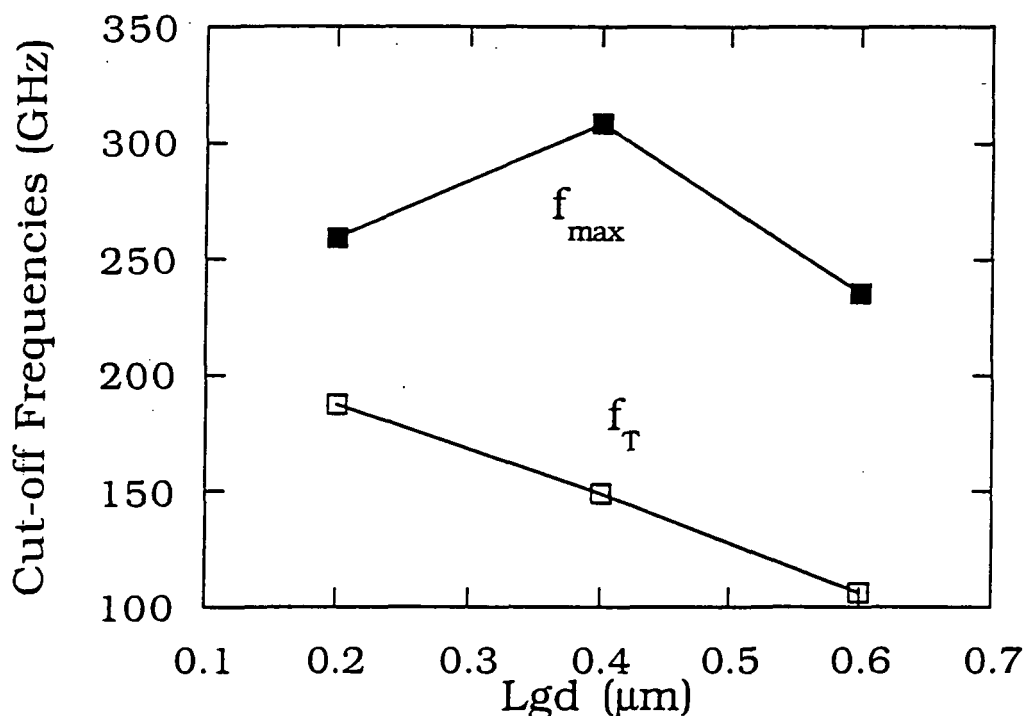


Figure 3: Microwave data of offset self-aligned InAlAs/InGaAs HEMT's ($L_{gd} = 0.4 \mu m$). The results show an f_T of 150 GHz and an f_{max} of 310 GHz, corresponding to a high f_{max}/f_T ratio of 2.0

drawback can, however, be eliminated by a better optimization of the doses used for the footprint and side lobes of the gate.

3 Evaluation of Oscillator Characteristics Using Large-Signal Analysis

The design of high frequency oscillators is generally based on either small-signal S-parameters or measured large-signal S-parameters. The small signal S-parameters predict the initial conditions necessary for oscillation build up. However, the steady-state oscillation condition can not be accurately predicted from small-signal S-parameters. Designs using measured large-signal S-parameters present also certain difficulties arising from measurement accuracy and differences between measured and simulated conditions.

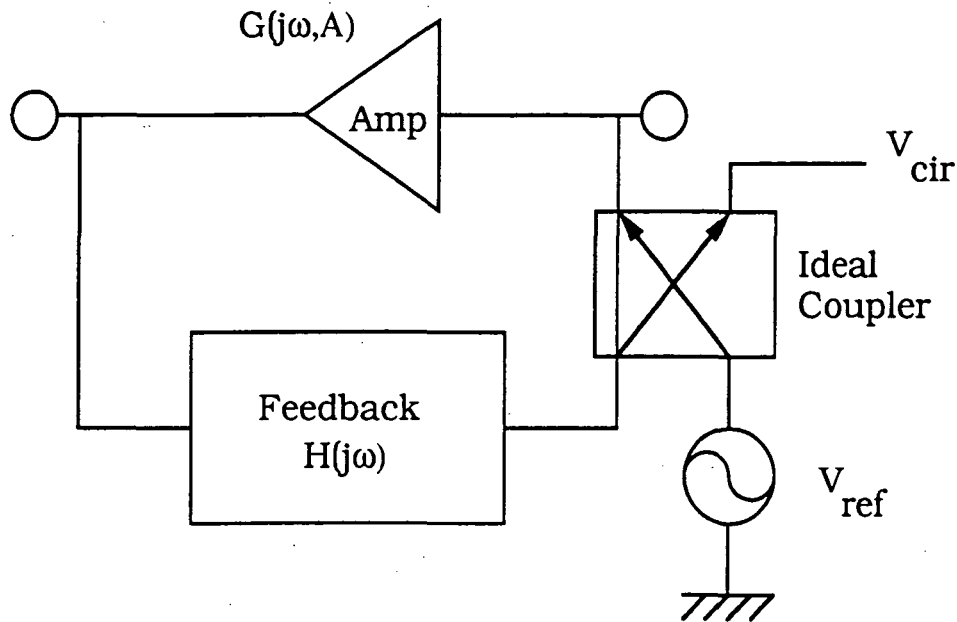


Figure 4: The schematic circuit setup for the large-signal oscillator analysis

An all frequency-domain large signal oscillator analysis method has been developed in view of evaluating the HEMT potential as oscillator. It employs small-signal S-parameters and a harmonic balance routine with 2-D interpolation functions. The method predicts the operation frequency, output power and optimum load termination conditions.

A special circuit set-up is used to perform the large-signal oscillator analysis (Fig. 4). It consists of an amplifying unit and frequency-selective feedback loop together with an excitation signal. The HEMT is used in common source topology and is considered as an amplifying unit with power-dependent gain saturation characteristics. An ideal coupler is placed between the amplifying unit and feedback loop to initiate and monitor the oscillation (V_{cir}). The excitation signal (V_{ref}) is increased from a small signal level until the gain of the HEMT saturates and the steady-state oscillation condition is reached.

The large-signal oscillator analysis method has been applied to study the oscillation power dependence on the termination impedance of common source InAlAs/InGaAs HEMT oscillators. The simulation results are shown in Fig. 5 for a HEMT with 2

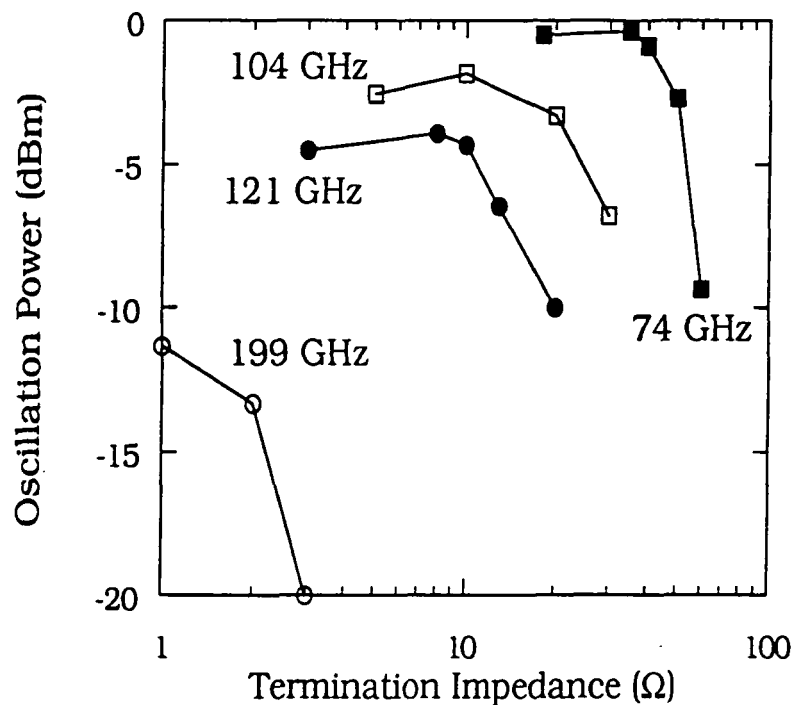


Figure 5: The oscillation power dependence on the termination impedance at various frequencies for a HEMT ($L_g = 0.1 \mu m$) with $f_{max} = 200$ GHz and gate periphery of $2 \times 45 \mu m$

$\times 45 \mu m$ gate periphery and f_{max} of 200 GHz. The analysis shows that an optimum output power level is obtained when the load impedance is of the order of $1/2$ to $1/4$ of the small signal negative resistance at frequencies which are sufficiently away from f_{max} . At very high frequencies, the load impedance determined by the above criteria is reduced to very small values (below 5Ω) which are difficult to implement in monolithic form. This termination load requirement sets the practical limit of upper frequency at which the oscillator circuit can be implemented. These effects were studied and design criteria were established on the basis of practical realization constraints imposed by load terminations which should exceed 5Ω .

The available power was evaluated at different frequencies using optimum termination

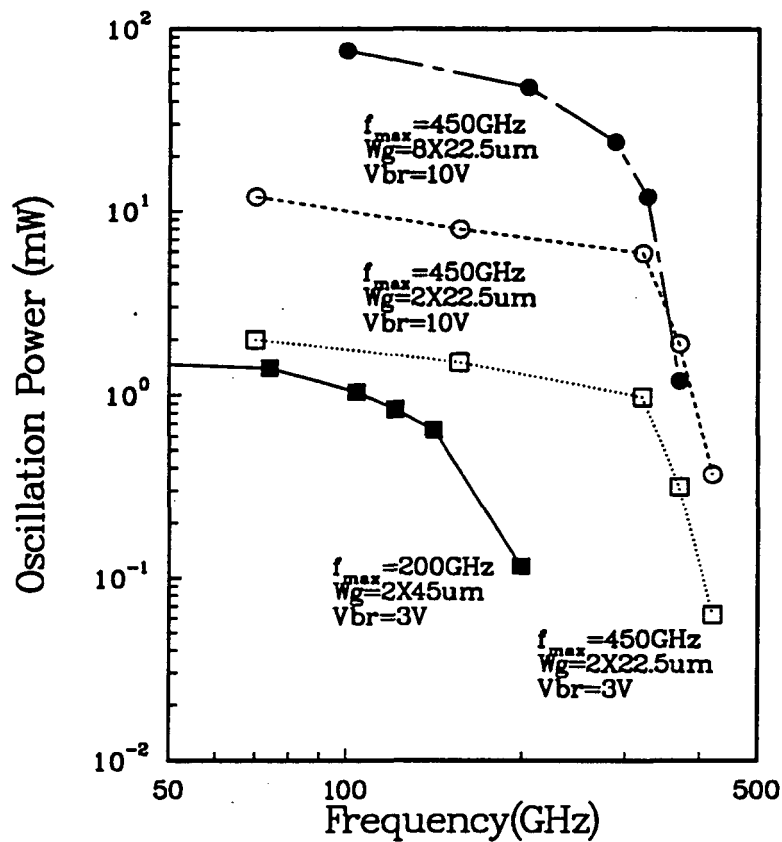


Figure 6: Power delivered by InAlAs/InGaAs HEMT oscillators as a function of frequency, gate periphery (W_g), maximum frequency of oscillation (f_{max}) and breakdown voltage (V_{br})

conditions. Three parameters are used for the simulation: gate periphery (W_g), maximum frequency of oscillation (f_{max}) and breakdown voltage (V_{br}). The results are shown in Fig. 6. The oscillation power decreases first slowly and shows a more dramatic degradation at high frequencies close to f_{max} . This corresponds to the degradation of maximum available gain (G_{max}) and negative resistance (R_{neg}) at high frequencies. The reduced R_{neg} imposes a smaller value of termination load with the result of less power delivered to the load. The overall characteristics suggest that generation of reasonable power levels is feasible up to a frequency of 2/3 of f_{max} . From Fig. 6, it is obvious that a higher f_{max} ensures large oscillation power for a given frequency. More than 15 mW of output power can be expected up to 300 GHz out of $0.1 \mu m$ HEMT's with eight 22.5

μm gate fingers assuming an f_{max} of 450 GHz and V_{br} of 10 V. This prediction doesn't include any parasitic effects coming from mismatches, losses of transmission lines and source grounding.

Fig. 6 also shows the characteristics of devices with different gate widths in view of studying the effect of gate periphery on the output power level. Larger devices provide higher oscillation power, but they are harder to implement in oscillator circuits. This is due to their lower induced negative resistance, which implies the need for very small termination impedance. As a result, the oscillation power degrades fast at the high frequency end of operation bandwidth. A compromise has consequently to be made between the oscillation power and ease of realization when choosing the device periphery.

Another important parameter in the oscillator evaluation is the breakdown voltage. A higher breakdown voltage allows one to bias the transistor at larger drain bias and thus to apply higher DC power to the device. The RF power generated from the device is proportional to the DC power and increases consequently with higher V_{br} . Under conditions of optimum biasing for power, the maximum voltage swing is $\sim V_{\text{br}}/2$. By increasing the breakdown voltage of the HEMT's from 3 V to 10 V, it was found that the RF power increased by approximately 6 dB. Breakdown improvements in InAlAs/InGaAs HEMT's have recently been reported by Matloubian et al [10] and validate this assumption. Further work is, however, necessary to justify this possibility, especially at millimeter-wave frequencies. Similar improvements can also be made by increasing the current density of the device and may be even easier to achieve in InAlAs/InGaAs HEMT's with the help, for example, of multi-heterojunction designs [11].

It should finally be noted that the simulation results in Fig.6 were obtained using a simple series feedback topology and the evaluated oscillation power values do not therefore necessarily reflect the maximum power capability of the devices.

Overall, the HEMT's can be optimized for generation of adequate power levels at

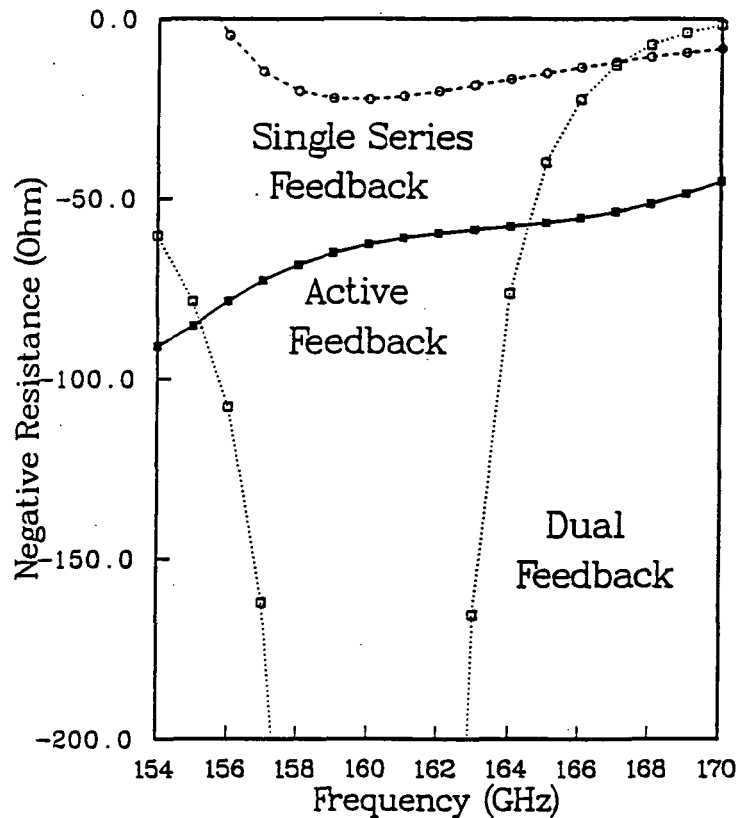


Figure 7: Comparison of negative resistance for three different feedback schemes: 1) single series feedback, 2) dual feedback, 3) active feedback

high frequencies with the help of: i) high f_{max} , ii) high V_{br} , iii) high current density, iv) choice of appropriate gate periphery.

4 Circuit Topologies for Subterahertz Monolithic HEMT Oscillators

As already discussed earlier on, the negative resistance available at subterahertz frequencies is usually rather small. Furthermore, the induced negative resistance is present over a narrow frequency range especially when the oscillation frequency is close to the f_{max} of the device. The availability of small negative resistance values make the design task very difficult. Therefore, appropriate topologies have to be selected such that the negative resistance can be maximized over a wide frequency range.

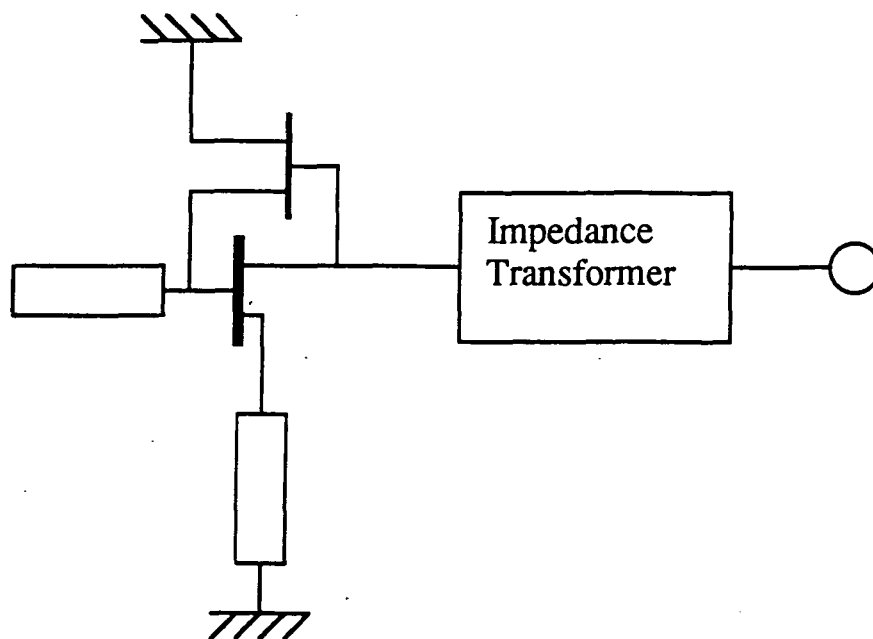


Figure 8: Equivalent circuit schematic of active feedback oscillator for subterahertz application

Dual feedback schemes can be used to improve R_{neg} over a narrow frequency range. In addition to the series feedback element from source to ground, a parallel feedback element can be inserted between the gate and drain. The negative resistance of this topology is compared with that of single series feedback topology in Fig. 7. As shown in this figure, dual feedback circuits provide the possibility of obtaining larger negative resistance. However, the negative resistance is present over a narrower range of frequencies than in the case of single series feedback circuits.

The active feedback approach is another alternative for designing oscillators with devices of small R_{neg} . It uses a small FET as a phase shifting element between the gate and drain (see Fig. 8). Since the feedback loop is provided by active rather than passive elements, the feedback phase shift is fairly independent of frequency and therefore oscillation is guaranteed over a wide range of frequencies. This can be verified from Fig. 7. Furthermore, the active feedback approach is less sensitive to the parasitics coming from passive elements and interconnects because it does not strongly depend on passive

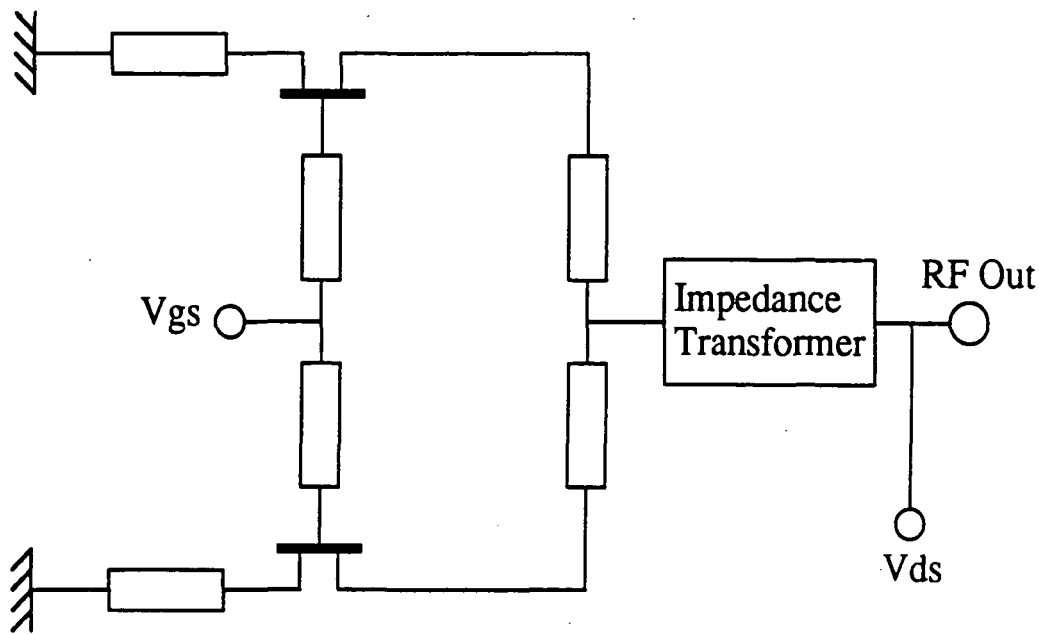


Figure 9: Equivalent circuit schematic of push-push feedback oscillator for subterahertz signal generation

circuitry for inducing the oscillation. It is therefore very suitable for high frequency circuit applications, where accurate modeling of passive circuit elements is not really available.

Another very interesting topology is the push-push configuration. The circuit schematic is shown in Fig. 9. It consists of two subcircuits combined in push-push arrangement. Each circuit oscillates at half the output frequency. The second harmonics are here combined in phase at the output terminal, while the first harmonics cancel each other. This configuration has the advantage of essentially doubling the operation frequency of the discrete devices. Thus, the circuit may operate beyond the frequency limit imposed by f_{max} . This topology also, provides the possibility of lowering the phase noise because all the odd harmonics and associated noise are canceled at the output. Good balance between the two subcircuits has to be maintained for the successful operation of this circuit, but mutual interaction between the two devices is expected to make this requirement less stringent. Monolithic technology provides additional means

of achieving perfect balance. The monolithic push-push HEMT oscillator is therefore a very promising candidate for satisfying the needs for subterahertz signal generation using HEMT's.

5 Conclusions

The use of submicron InAlAs/InGaAs HEMT technology has been discussed in view of the possibility of realizing subterahertz oscillators. InP-based HEMT's have been optimized for this purpose and showed very high f_{max} of 310 GHz using offset self-aligned Γ -gate technology. A gate-to-drain separation of $0.4 \mu m$ was used in these devices.

A large signal modeling method has been developed and applied to the evaluation of power characteristics of HEMT oscillators. The optimum termination loads have been found to be $1/4 - 1/2$ of the small-signal negative resistance of the devices. Upper frequency limit criteria have been established and indicated the feasibility of signal generation up to $\sim 2/3$ of the f_{max} of the device. The large signal analysis has also been used to evaluate the oscillation power of HEMT oscillators in the subterahertz region. The use of HEMT's with $f_{max} = 450$ GHz, $V_{br} = 10$ V and $W_g = 8 \times 22.5 \mu m$ should allow an oscillation power of 15 mW at 320 GHz.

The topology study of subterahertz oscillation has shown that enhanced negative resistance can be obtained by using complex feedback schemes such as the dual feedback and active feedback scheme. The frequency barrier imposed by f_{max} can be overcome by harmonic oscillation operation as for example in the case of push-push oscillators.

Acknowledgment

The help of T. Brock, G. Munns and G. I. Ng in technology and material growth are greatly appreciated.

References

- [1] L. D. Nguyen, A. S. Brown, M. A. Thompson, L. M. Jelloian, L. E. Larson, and M. Matloubian, "650-Å Self-Aligned-Gate Pseudomorphic $\text{Al}_{0.48}\text{In}_{0.52}\text{As}$ / $\text{Ga}_{0.20}\text{In}_{0.80}\text{As}$ High Electron Mobility Transistors," *IEEE Electron Dev. Lett.*, vol. 13, no. 3, pp. 143–145, March 1992.
- [2] P. Ho, M. Y. Kao, P. C. Chao, K. H. G. Duh, J. M. Ballingall, S. T. Allen, A. J. Tessmer, and P. M. Smith, "Extremely High Gain 0.15 μm Gate-Length $\text{InAlAs}/\text{InGaAs}/\text{InP}$ HEMTs," *IEE Electron. Lett.*, vol. 27, pp. 325–327, 1990.
- [3] Y. Kwon, D. Pavlidis, P. Marsh, G. I. Ng, and T. Brock, "Experimental Characteristics and Performance Analysis of Monolithic InP -Based HEMT Mixers at W-Band," *To appear in IEEE Trans. Microwave Theory Tech.*, 1992.
- [4] Y. Kwon, D. Pavlidis, P. Marsh, M. Tutt, G. I. Ng, and T. Brock, "180GHz $\text{InAlAs}/\text{InGaAs}$ HEMT Monolithic Integrated Frequency Doubler," in *Tech. Digest of 1991 IEEE GaAs IC Symposium*, pp. 165–168, October 1991.
- [5] Y. Kwon and D. Pavlidis, "Large Signal Analysis and Experimental Characteristics of Monolithic InP -Based W-Band HEMT Oscillators," in *Proceedings of the 21st European Microwave Conference*, pp. 161–166, September 1991.
- [6] Y. Kwon, D. Pavlidis, and M. N. Tutt, "An Evaluation of HEMT Potential for Millimeter-Wave Signal Sources Using Interpolation and Harmonic Balance Techniques," *IEEE Microwave and Guided Wave Letters*, vol. 1, pp. 365–367, December 1991.

- [7] U. K. Mishra, A. S. Brown, L. M. Jelloian, M. Thompson, L. D. Nguyen, and S. E. Rosenbaum, "Novel High Performance Self-Aligned 0.15 Micron Long T-Gate," in *Tech. Digest of 1989 International Electron Device Meeting*, pp. 101-104, December 1989.
- [8] M. B. Das, "A High Aspect Ratio Design Approach to Millimeter-Wave HEMT Structures," *IEEE Trans. on Electron Devices*, vol. ED-32, no. 1, pp. 11-17, January 1985.
- [9] Y. Kwon, T. Brock, G. I. Ng, D. Pavlidis, G. O. Munns, M. E. Sherwin, and G. I. Haddad, " F_{max} -Enhancement in CBE-Grown InAlAs/InGaAs HEMT's Using Novel Self-Aligned Offset-Gate Technology," in *4th Conf. on InP and Rel. Materials*, April 1992.
- [10] M. Matloubian, L. D. Nguyen, A. S. Brown, L. E. Larson, M. A. Melendes, and M. A. Thompson, "High Power and High Efficiency AlInAs/GaInAs on InP HEMTs," in *1991 IEEE Int. Microwave Symp. Dig.*, pp. 721-724, June 1991.
- [11] G. I. Ng, D. Pavlidis, M. Tutt, J.-E. Oh, and P. K. Bhattacharya, "Improved Strained HEMT Characteristics Using Double-Heterojunction $\text{In}_{0.65}\text{Ga}_{0.35}\text{As} / \text{In}_{0.52}\text{Al}_{0.48}\text{As}$ Design," *IEEE Electron Dev. Lett.*, vol. 10, no. 3, pp. 114-116, March 1989.